

The strength of hybrid glass/carbon fibre composites

Part 2 *A statistical model*

P. W. MANDERS, M. G. BADER

Department of Metallurgy and Materials Technology, University of Surrey, Guildford, UK

When carbon fibre is combined with less-stiff higher-elongation glass fibre in a hybrid composite an enhancement of the failure strain of the carbon fibre reinforced phase is observed. This "hybrid effect" is only partially accounted for by internal compressive strains induced by differential thermal contraction during fabrication. The predominant factor is shown to be a relationship between the strength and effective bundle size of the carbon fibre ligaments which is a consequence of the statistical distribution of strength-reducing flaws in the carbon fibres. A lamina or ligament (bundle) of carbon fibres fails when there is a local critical accumulation of fibre fractures. A model based on this concept is used to relate the two-parameter Weibull strength distribution of the carbon fibre reinforced composite phase to that of single carbon fibres. The model suggests that the critical number of fibre fractures is of the order of 3, and experimental observations of the failure process support this hypothesis.

Nomenclature

CFP carbon fibre reinforced phase.
 cfrp carbon fibre reinforced plastic.
 grp glass fibre reinforced plastic.
 Γ gamma function.
 σ stress.
 P probability.
 w Weibull shape parameter.
 σ_0 Weibull scale parameter.
 L length.

m number of links in a chain of bundles.
 n number of fibres in a bundle.
 i number of fibre fractures in a group which leads to catastrophic fracture.

Subscripts

f failure.
 s survival.
 m chain of m links.
 n bundle of n fibres.
 L links of length L .

1. Introduction

In a previous paper [1] we described the mechanical properties and macroscopic aspects of the failure of a range of glass/carbon fibre epoxy hybrid composites. In this paper we present observations of the micromechanisms of failure and relate these to a model of composite failure based on the statistics of fibre fracture. The major finding of the previous work is that the failure strain of the carbon fibre reinforced phase (CFP) of the hybrid is not constant, but depends on the geometrical distribution of the two types of reinforcing fibre. As a general rule, the apparent

failure strain of the CFP increases as the discrete ligaments of CFP are reduced in size, and as the ratio of glass to carbon fibre is increased. Part of this failure strain increase can be accounted for by differential thermal contractions which resulted in a compression of the CFP when the composites were cooled after curing. However, the remainder of the increase, and its variation with the size of the CFP (at constant ratio of glass to carbon fibre), are unexplained. It is the purpose of this paper to show how a statistical model of failure can account for that part of the hybrid effect which is not of thermal origin. In addition we relate the

strength of the CFP in the hybrids to the strength distribution of single carbon fibres tested in isolation.

First we discuss fracture mechanical (thermodynamic) and micromechanical (statistical) approaches to understanding the failure of a composite containing a single type of fibre, and suggest two ways in which combining fibre types might lead to an enhancement of the failure strain of the lower elongation fibre.

The fracture mechanics approach is essentially concerned with the strength of a flawed structure which fails by propagation of a pre-existing crack when conditions at the crack tip become thermodynamically favourable. Application to fibre reinforced composites in the case of fracture perpendicular to the fibres is complicated by the fact that the material is both structurally inhomogeneous and anisotropic in its elastic and fracture properties. Although both the matrix and fibre are brittle solids, typical fractures do not involve a single crack with smooth surfaces, but rather a microscopically tortuous fracture path with matrix cracks linking fibre fractures, often also with debonding between fibre and matrix, (Figs 1 and 2) often extending several fibre diameters on either side of a fibre fracture. If fracture mechanics are to have a valid application at the macroscopic level, the crack-tip zone should be sufficiently large for the material there to behave in an effectively homogeneous manner, which means that the crack should be very large in comparison with the fibre diameter. This effectively precludes the use of fracture mechanics to explain the intrinsic strength of cfrp at the macroscopic level, because, as fabricated, composites do not contain cracks of such a size.

Typically cfrp can be expected to contain a range of stress-concentrating defects, associated with the fibres themselves (e.g. weak points caused by inclusions, porosity and surface features [2]), or introduced during composite fabrication, (e.g. broken fibres, misaligned bundles and uneven distribution of fibre [3]). In a well-made composite fabrication defects are of secondary importance to the fibre defects which precipitate the failure of individual fibres as the composite is loaded. Conceptually there is no bar to applying fracture mechanics analysis to the fibre defects, taking into account the microstructural inhomogeneity. Typically the first failure of a fibre does not lead to ultimate failure of the composite

because the weak fibre–matrix interface arrests the crack by debonding. However, there is a local stress perturbation around a fibre fracture which leads to a stress intensification in neighbouring fibres so that they will tend to fail at lower levels of applied stress. Continued propagation of a crack beyond the first failure of a fibre is a statistical problem involving the distribution of weakness in the adjacent fibres.

Statistical theories of composite failure, e.g. [4–15], generally assume that all fibres in a composite are nominally identical, and initially uniformly stressed, so that a fibre will fail at its weakest point by propagation of a flaw when a critical value of stress is reached. Fibres of a given length will exhibit a scatter of strengths on account of the random distribution of strength-limiting flaws, and their median strength will decrease with increasing length as each fibre will have a greater probability of containing a flaw of a given severity. The Weibull distribution is a reasonable description of the strength distribution of single fibres tested in isolation (e.g. Fig. 3) and is commonly adopted for its mathematical convenience. The models in references [4–15] consider a composite to consist of a chain of bundles of fibres (Fig. 4) and relate the strength distribution of the fibre to that of a short bundle. It is then a simple matter to obtain the strength distribution of the composite as a chain of such bundles. A key feature of many statistical models is that the median strength of a composite decreases as its bulk size is increased, by increasing the length or cross-section (number of fibres), since in the greater volume of material there is a higher probability of a catastrophic sequence of fibre fractures, leading to ultimate failure, at any given applied stress.

The thermodynamics (fracture mechanical) and statistical approaches to composite strength are compatible because fracture mechanics considers either a very large crack with a large damage zone at its tip in which statistical effects are insignificant, or is applied at the microscope level where statistical variations between fibres dominate. Statistical models adopt experimentally determined distributions for fibre strength in which thermodynamic conditions for fibre fracture are obviously met. (The matrix is assumed to have negligible strength in the fibre direction.) However, it should be noted that these distributions are usually determined for isolated fibres, whereas in a composite, fibre flaws are elastically coupled via the matrix to

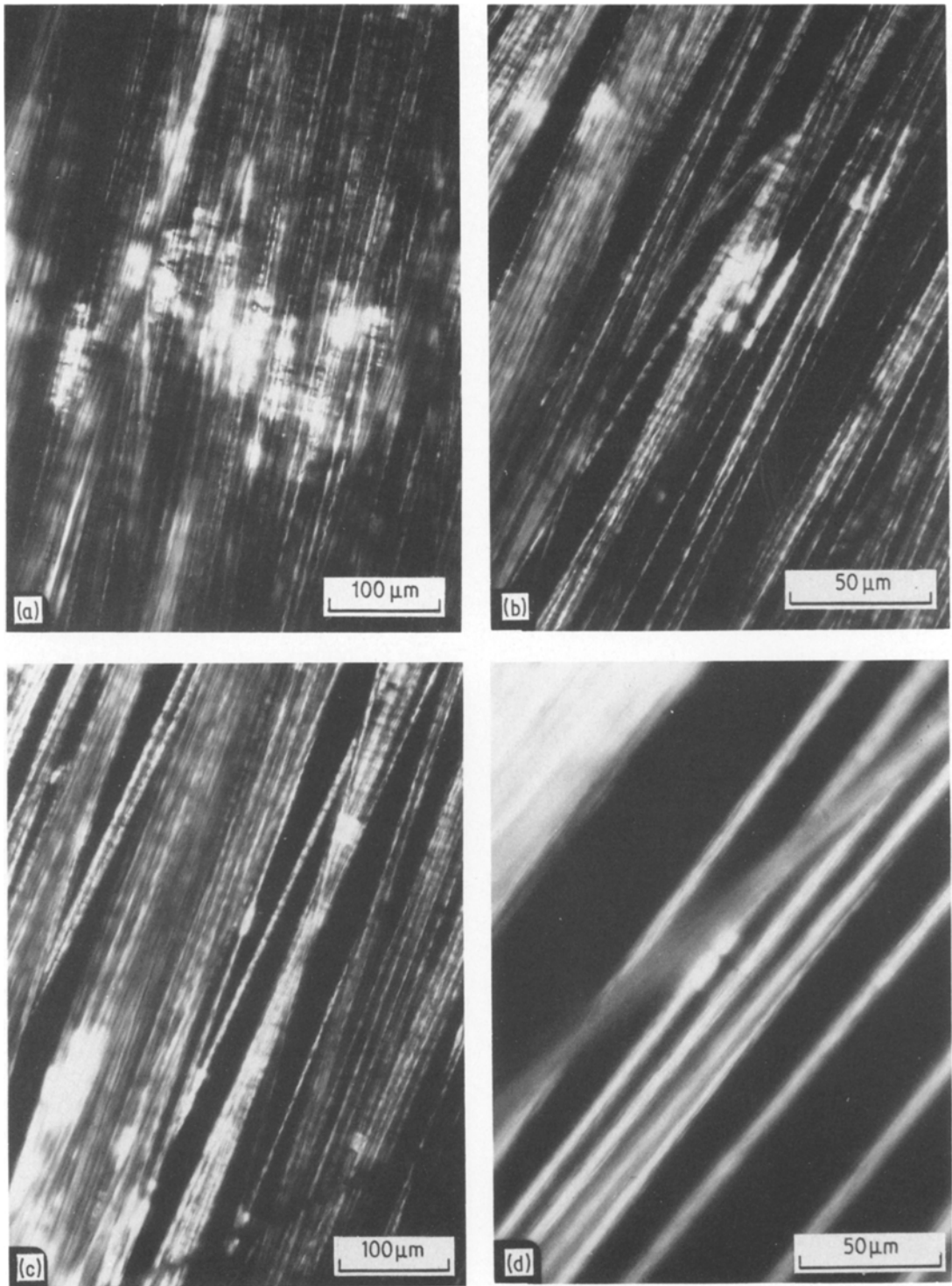


Figure 1 Photomicrographs of the carbon fibre layer of a spread-tow hybrid strained to 0.02, taken in polarized light to show up the debonding between fibre and matrix (lighter areas). (a) Large group of carbon fibre fractures; (b) intermediate group of carbon fibre fractures; (c) isolated carbon fibre fractures; (d) a pair of adjacent fibre fractures, only one of which is debonded.

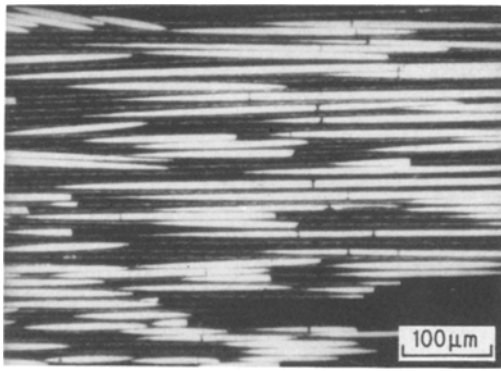


Figure 2 Section of the carbon fibre layer in a spread-tow hybrid strained to 0.02.

adjacent (stiff) fibres, and may therefore propagate at different applied stresses.

It is easy to see how a hybrid effect can exist on a statistical model. The smaller the volume of cfrp in a discrete ligament, the higher will be its failure strain, and so long as the glass fibre is effective in preventing the propagation of fractures from bundle to bundle, the cfrp in a hybrid will exhibit a greater average failure strain than a similar volume in an all cfrp composite.

In a fracture mechanics model a hybrid effect can arise as follows. When a composite is stressed fibre fractures occur, initially at random, but later preferentially in the overstressed zones surrounding previous fibre fractures. Ultimately a group of fractures reaches a critical size and catastrophic crack propagation occurs. Although this group of fibre fractures may be too small for rigorous application of fracture mechanics, the principles remain the same. Thus, as the applied stress is increased the inherent flaw size (i.e. groups of failed fibres) increases, whilst the critical flaw size will decrease as a consequence of the increased strain energy density [8, 9]. Consider now a defect shown as a "crack" in an all-carbon fibre ligament,

Fig. 5a. It will propagate at some critical applied stress (or strain). If, however, the same ligament containing the same crack were part of a hybrid, shown in Fig. 5b, the crack would be bridged by glass fibres. This would reduce the rate of strain energy release as the crack grew and a higher applied stress (or strain) would be required to propagate the crack in the ligament. This concept will be termed "constraint".

Both of these models for the hybrid effect are based on the assumption that the glass fibre phase does not fail. The practical requirement for the realization of this condition is that no significant number of glass fibres should fail in the region of stress intensification close to fractures in the CFP. In the early stages of failure this requirement is easily met, since the failure strain of the glass fibre is more than twice that of the carbon. However, as the CFP fails, load is redistributed onto the glass fibre, until it also fractures. The range of strain between the onset of CFP failure and of ultimate failure depends on the relative volumes and moduli of the two phases.

In the present work we have attempted to explain the hybrid effect on the basis of the statistical strength of the carbon fibres. Experimental data have been gathered from a series of tests in model hybrid composites, in which the carbon fibre ligament size has been systematically varied. This work is described in Part 1 [1] of this paper. The dependence of the probability of ligament failure on size and strain has been determined, and further evidence in support of the proposed model of failure has been gathered from an extensive programme of microscopy.

2. Discussion

2.1. Strength of single fibres

Later discussion of the strength of cfrp will involve the strength distribution of single carbon fibres of

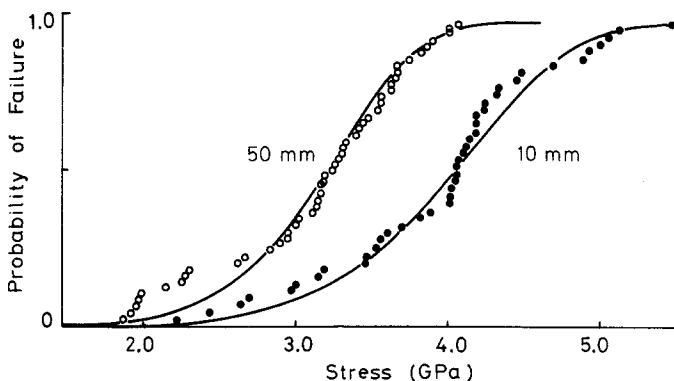


Figure 3 Strength distributions for HTS carbon fibres of two gauge lengths with fitted Weibull functions.

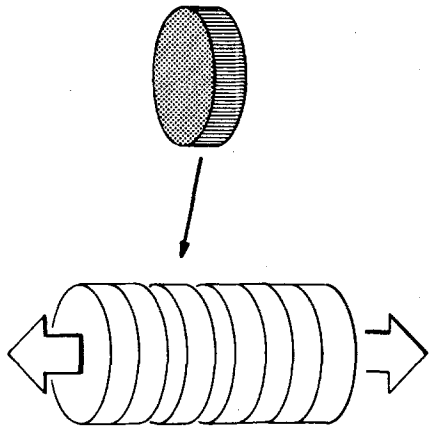


Figure 4 Chain-of-bundles model of a unidirectional fibre composite.

the order of $100\ \mu\text{m}$ in length. It is impractical to measure the strength of such lengths directly without specialized equipment. However, the strength distribution was measured at 50 and 10 mm, and was found to approximate to a Weibull distribution which allowed extrapolation to predict the strength at shorter gauge lengths. Fifty HTS carbon fibres (from the same production batch as used for the spread-tow and divided-tow hybrids) were selected from all parts of the tow and tested to failure. The diameter of each fibre was measured by laser diffraction to within $\sim 2\%$. The failure stresses were

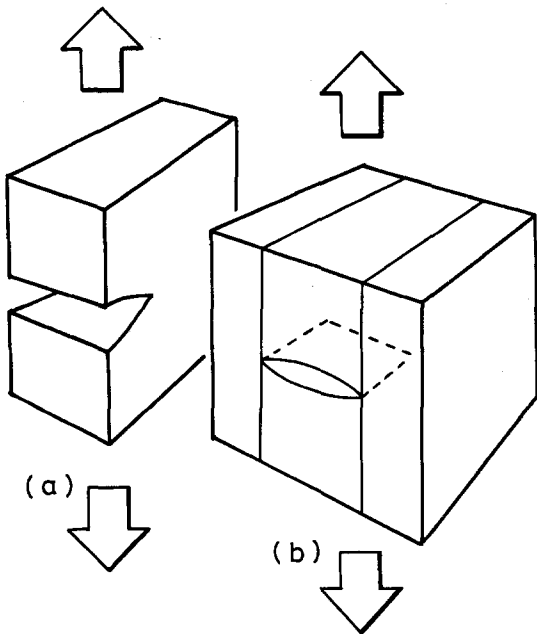


Figure 5 The principle of "constraint" in hybrid laminates: (a) unconstrained crack; (b) crack in one ply constrained by uncracked adjacent plies.

plotted as cumulative probability distributions, Fig. 3, and were fitted to a two-parameter Weibull distribution

$$P_f = 1 - \exp \left[-L \left(\frac{\sigma}{\sigma_0} \right)^w \right]. \quad (1)$$

The Weibull scale and shape parameters were found to be $\sigma_0 = 2.17\ \text{GPa}$ and $w = 6.98$, respectively.

2.2. "Weakest link" aspect of fibre strength

In the introduction it was argued that a composite would show a size effect in its strength if ultimate failure was determined by some sequence of events whose probability of occurrence at a given stress depended on the volume of material stressed. In a single fibre it is easily seen how such behaviour arises. Consider a length of fibre L whose strength distribution is given by Equation 1. If m such lengths are chained together to give a fibre mL long, its strength will be determined by the weakest length in the chain. The probability of survival of the chain is the product of the probabilities of survival of each constituent length.

$$P_{smL} = (P_{sL})^m. \quad (2)$$

Also

$$P_f = 1 - P_s, \quad (3)$$

so, from Equation 1,

$$P_{fmL} = 1 - \exp \left[-mL \left(\frac{\sigma}{\sigma_0} \right)^w \right]. \quad (4)$$

Note that in Equation 4 the strength decreases with increasing length, but the parameter w which is an inverse measure of the spread in strengths remains the same (Equation 6). Coleman [4] considers in detail the variation of fibre strength with length using the Weibull distribution. The median strength is given when $P_f = P_s = 0.5$. Mean strength is given by

$$\left(\frac{\bar{\sigma}}{\sigma_0} \right) = L^{-1/w} \Gamma \left(1 + \frac{1}{w} \right) \quad (5)$$

and the coefficient of variation by

$$\left[\frac{\Gamma(1 + 2/w)}{\Gamma^2(1 + 1/w)} - 1 \right]^{1/2} \quad (6)$$

(see Coleman [4]).

Size-dependent behaviour of the strength of a single fibre is conveniently displayed in a graph of $\ln \sigma$ against $\ln L$, (at constant probability of failure). From Equation 1 this is seen to be linear with gradient $-1/w$.

Thus plotting $\ln(\text{median strength})$ against $\ln(\text{length})$ gives a straight line with gradient of $-1/w$. Similarly, plotting $\ln(\text{mean strength})$ against $\ln(\text{length})$ also gives a line of gradient $-1/w$ from Equation 5. Use of a Weibull probability plot in this way is described by Harlow and Phoenix [15]. We use the $\log(\text{strength})$ against $\log(\text{length})$ plot as a test of Weibull behaviour.

2.3. The "chain of bundles" model for the strength of a composite

In a composite conceived as a chain of m bundles each of n fibres in parallel, see Fig. 4, ultimate failure occurs at the first failure of a bundle. An equation analogous to Equation 4 may be written for the strength distribution of the composite in terms of the strength distribution of a bundle. For a given size of bundle, say n fibres, we expect weakest-link behaviour with a shape parameter w_n . However, such an equation does not relate the strength distribution of the composite to that of a single fibre. Indeed, relating the strength distribution of a bundle of n fibres to that of a single fibre is a complex problem whose rigorous solution has met with only partial success. Harlow and Phoenix [15] review various approaches to the problem. The complexity arises as follows: To calculate the probability of failure of a bundle at any given applied stress, it is necessary to determine all possible sequences of fibre fractures which lead to failure. The probabilities of each sequence occurring at a given stress are summed to give the probability of failure of the bundle. The probabilities of each failure sequence must be expressed in terms of fibre failure probabilities, taking into account the complex geometry and redistribution of load which occurs when a fibre fails.

The "chain-of-bundles" model of failure in a composite has been considered in [5–15]. These approaches differ chiefly in the assumptions made about the redistribution of load at fractures and in the failure criteria adopted. Of particular relevance here are the approaches of Zweben and Rosen [6–11] and Harlow and Phoenix [15] who examine the case where load formerly carried by a broken fibre is concentrated on a small number of adjacent fibres. Harlow and Phoenix [15] adopt a local load sharing rule which considers only nearest neighbours, whereas Zweben and Rosen [6–11] consider more distant fibres. The load is generally assumed to be evenly distributed over some

"ineffective length" of these fibres, though this is most unlikely to be the case in reality. Three failure criteria are of particular interest: Gücer and Gurland [5] adopt a first-fibre fracture criterion which we discuss below, while Zweben and Rosen [6–11] adopt first failure of an overstressed fibre. Harlow and Phoenix [15] consider all sequences of fibre failures (for a composite of small size < 9 fibres). More recently Batdorf [16], Smith [26], and Harlow and Phoenix [27] have considered the critical size of a group of fibre fractures. In all cases the critical number of adjacent fibre fractures is small, of the order of 3, which agrees well with our experimental observations. These analyses explicitly relate w for a fibre to w_n for a bundle.

2.4. Weakest link aspects of composite strength

The simplest failure criterion for a bundle of n fibres bonded together is that the first fibre failure propagates through all the fibres. In this case a fibre fracture constitutes a "weakest link" in the structure and an expression analogous to Equation 4 can be written

$$P_{fn} = 1 - \exp\left[-n\left(\frac{\sigma}{\sigma_0}\right)^w\right] \quad (7)$$

for a bundle of n fibres and unit length, L . Similarly for a chain of m bundles of n fibres

$$P_{fmn} = 1 - \exp\left[-mn\left(\frac{\sigma}{\sigma_0}\right)^w\right]. \quad (8)$$

Equation 8 plots as a straight line of gradient $-1/w$; the same as for single fibres, in a graph of $\ln(\text{strength})$ against $\ln(\text{size})$, see Fig. 6, where composite size is measured in terms of the *total* length of fibre, (mn) i.e. a measure of *volume*. This is not surprising, since it is the same event which causes failure in both single fibre and composite.

Our experimental observations indicate that the first failure of a carbon fibre does not result in complete failure of the bundles but that failure of a small group of i fibres does, see the Appendix. For a large bundle of fibres ($n \gg i$) it is reasonable to adopt failure of i adjacent fibres as a valid failure criterion. This assumption avoids the necessity of calculating all failure sequences, and Harlow and Phoenix [15] whose computed model has done this, argue that over a fairly wide range of composite size, when n is large, failure has weakest-link characteristics, (evidenced by a rela-

tively straight portion of their $\ln(\text{strength})$ against $\ln(\text{size})$ graph).

Batdorf [16], Smith [26] and Harlow and Phoenix [27] show that the dependence of the probability of failure of the composite on stress is to the power iw , whereas it is w in the case of a single fibre, or fracture of a composite following the first fibre fracture.

Harlow and Phoenix [15] give an example based on their predictions in which w_n for a realistic composite is about 4.5 times that of a single fibre ($w = 5$, $mn \approx 10^6$). This indicates that a critical group of 4 to 5 fibre fractures would be required for catastrophic failure.

2.5. Weibull behaviour of hybrid composites

To test whether the cfrp is hybrid composites exhibits "weakest link" type behaviour its strength was plotted against the volume of fibre on the logarithmic axes of Fig. 6. Gradients of the lines for cfrp and single fibres were compared to give an indication of the value of i .

In the case of the all-carbon and laminated hybrids this was simply accomplished by plotting the nominal fibre failure stress (calculated from the cfrp failure strain after correction for residual thermal strain) against the total volume of carbon fibre in the CFP. The single fibre results were plotted in a similar manner.

However, the divided-tow results were manipulated in the manner described in Part 1 [1] to allow for the volume of material relieved of stress by debonding at each fracture of the carbon ligament.

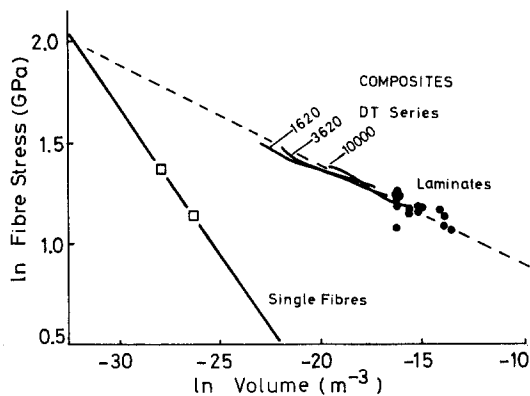


Figure 6 Relationship between mean strength of the carbon fibre ligament and its total volume of fibre (HTS fibre). The failure stresses have been adjusted for residual thermal stresses.

The mean fibre stress at each successive crack was plotted against the "true" mean volume of material under test, for bundles of 10 000, 3620, 1620 and 620 fibres, as the solid curves in Fig. 6.

A straight line may be drawn through all the composite data in Fig. 6, which it should be noted, span a range of >1000 in volume. Over this volume range the strength against size behaviour is consistent with a Weibull statistical model of failure. The gradient of this line is -0.043 , showing a much smaller decrease in strength with volume than is the case with single fibres where the gradient is -0.145 . These gradients indicate Weibull shape parameters of ~ 7 and 23 for single fibres and the CFP respectively, from which we deduce that i is ~ 3 fibres. This is consistent both with experimental observations and the model developed by Harlow and Phoenix [15].

A fracture mechanics approach is not appropriate when a crack involves such a small number of fibres since its behaviour is dominated by the local microstructure. However, this does not mean that energetic aspects of fracture are unimportant. Aveston and Sillwood [17] estimated the failure strain of a single carbon fibre when it is embedded in grp. Their model equated the strain energy released from the fibre and surrounding matrix material (assumed to have the average properties of grp) when the carbon fibre failed, to the energy required to create the new fracture surfaces. This gave a thermodynamic lower bound for the failure strain of the fibres, which is higher when the fibre is "constrained" by relatively high modulus material (grp) than when the fibre is tested in isolation. Their estimated failure strains (for the two cases where the fibre remains bonded to the matrix, and where it debonds) are close to those they observed in a hybrid similar to the spread-tow hybrid discussed in Part 1 [1]. This suggests that fracture energetics could be a significant factor in determining the failure strain of fibres in a composite. Unfortunately they did not compare the strengths of the fibres in the hybrid, with those of fibres tested alone.

Bader and Manders [18] applied a similar energy balance equation to the laminated hybrids and again showed that the energy release is very similar to the energy requirement of the fracture surfaces. The implications of these results for the application of a statistical model of composite strength to hybrids are:

- (1) The distribution of fibre strength deter-

mined by single fibre tests may not be applicable when they are incorporated into a composite since they are effectively “constrained” by adjacent material.

(2) The size of a critical group of fibre fractures may depend on both the number of fibres in the bundle, and on the stiffness of the material surrounding (and constraining) the bundle.

3. Implications of “weakest link” type failure for the design of hybrid composites

3.1. Failure strain enhancement of cfrp

The most obvious consequence of “weakest link” type failure in cfrp is that it allows us to increase the effective strength of the carbon fibre simply by reducing the number of fibres in each bundle. Consider two unidirectional hybrid composites of similar dimensions, in which bundles of carbon fibre are separated by glass fibre. Hybrid A contains tows of 10^4 carbon fibres effectively isolated from each other by the grp while hybrid B contains bundles of only 10 carbon fibres similarly isolated. The Weibull shape parameter for the cfrp is 20 (a typical value for the type of material studied here). If the median strength of the 10^4 fibre bundles is say 1 GPa, the median strength of the bundles of 10 fibres (of the same length) will be 1.41 GPa, an increase of over 40%. The smaller bundles continue to contribute stiffness to the hybrid at much higher strains. The median strength of bundles of intermediate size is shown graphically in Fig. 7.

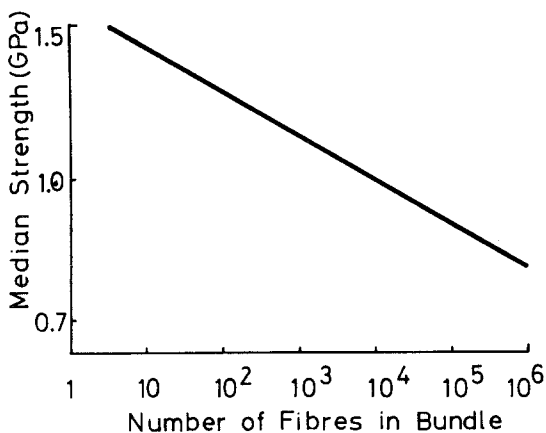


Figure 7 Relationship between median strength and bundle size for a hypothetical fibre composite with Weibull shape parameter of 20.

3.2. Load—strain behaviour

Further benefits ensue from this reduction in bundle size. The fractures of the cfrp are smaller and more evenly distributed throughout the composite, and the smaller delaminations between cfrp and grp will be less detrimental to the interlaminar shear strength. In addition the loss of load bearing capacity of the cfrp occurs as a large number of smaller events leading to a more gradual loss of modulus (at higher strains). The volume of cfrp which effectively ceases to bear load at each fracture depends on the debonding between the cfrp and grp and is a function of both the geometry (bundle size) and matrix strength.

3.3. What is the optimum state of dispersion?

If a cross-section of a bundle of n fibres contains a critical group of i fibre fractures, all fibres on that cross-section fail. The number of fibres which are caused to fail, and would not otherwise fail is $n - i$, and to achieve optimum utilization of the fibre this number should be as small as possible.

When $n \gg i$, reduction of n by a given factor increases the median strength by a (different) constant factor. This is a consequence of the approximately linear relationship between $\ln(\text{strength})$ and $\ln(\text{volume})$. In the example given in Section 3.1, reducing the bundle size by a factor of 2 increases the median strength by a factor of 1.035 (or 3.5%).

When n is close to or less than i reduction of the bundle size is less effective since the failure mode will no longer be by catastrophic propagation of a brittle crack. However, a marginal increase in strength can be expected from the effective reduction of over stresses around fibre fractures.

3.4. What is the optimum choice of fibres and their ratio?

Strength enhancement of the low-elongation fibre by reducing its bundle size relies on the effective isolation of these bundles by the higher elongation fibre which acts as a crack-arrest barrier. Thus, the strength distributions of the two fibres must be well separated for there to be negligible probability of a low-elongation fibre fracture causing failure of a high-elongation fibre, or vice versa, the necessary separation of scale parameters (σ_0) will depend on the shape parameters w , and also on the overstress on fibres near fibre fractures. The overstress depends in turn on the matrix and fibre strength

and modulus [19–22] and also dynamic factors [19]. Practically, carbon/glass, and carbon/Kevlar, combinations where the failure strains differ by a factor of about 3, are effective.

The ratio of low-elongation to high-elongation fibres is a major factor determining the shape of the load–strain curve since it governs the amount by which the hybrid extends when a bundle of low-elongation fibres fails. It also governs the partition of residual thermal strain between the high- and low-elongation phases. To obtain any benefit from a reduction of the low-elongation bundle size there must be enough high-elongation fibre present to ensure the mode of failure is by isolated fractures of fibre bundles. As long as this condition is satisfied the fibre ratio may be chosen to give the desired modulus, ultimate strength and rate of modulus decrease as the low-elongation fibre fails.

Many factors determine whether or not a fracture will propagate from (low-elongation) bundle to bundle, among them the ratio of fibre types, and the geometry of the bundles. Prediction of the strength of such an array is essentially the same problem as the array of fibres which we have considered here. Zweben [23] discusses hybrids in which fracture propagates readily between bundles, but in our experience the ultimate failure of glass–carbon hybrids involves multiple shear cracks in the fibre direction, and the composite would normally be considered unserviceable at an earlier stage of failure. Although the behaviour of arrays of bundles and fibres may be similar, different criteria of failure may apply to each.

Acknowledgements

Carbon fibre for this work was kindly provided by Courtaulds Ltd. One of us (PWM) is grateful for financial support from contributions made by British Aircraft Corporation Ltd (now British Aerospace) to the University of Surrey appeal funds.

Appendix

Optical microscopy of fibre failures

Two novel techniques were developed for the observation of fibre fractures in the hybrid composites described in Part 1 [1]. Carbon fibre fractures were observed directly through the outer plies of grp by using a low-power oil-immersion objective and top illumination [24]. Polarized light greatly increased the contrast since carbon fibre

surfaces are optically anisotropic, and with correct orientation will give a bright reflection, as seen in Fig. 1 (the streaks are due to surface fluting of the fibre). A further advantage of this technique is that it distinguishes areas of debonding between fibre and matrix where there is increased reflection. Fibre fractures are seen as fine dark lines across the fibres, and there is frequently debonding either side for several fibre diameters. Fig. 1 is a series of micrographs of a spread-tow [1] hybrid strained to 0.02 showing (a) a large group of fractures (b) several medium sized groups (3 to 10 fibres) and (c) isolated single fractures. Fibre fractures are not always accompanied by debonding and Fig. 1d illustrates this with two adjacent fractures, only one of which has debonding. This spread-tow hybrid was also sectioned and polished in the conventional manner at a small angle ($\sim 15^\circ$) to the fibre direction. Fig. 2 is a micrograph of a large group of fibre fractures in such a section. Fibre fractures are seen as dark lines across the fibres where the fibre is retained in the matrix on each side of the fracture. However, because of the oblique angle of section, some fibres rise out of the surface, and where they have debonded from the matrix they are lost from the surface during polishing. In this case the fibre fracture is indicated by a square, as opposed to elliptical profile at the end of the fibre.

Because it relies on the transparency of the grp plies in a hybrid specimen, the through-surface microscopy could only be usefully applied to spread-tow hybrids. For this reason a second technique was developed which examined transverse sections of composite. Electrolytic etching was used to decorate the ends of conducting carbon fibres in a thin polished slice of composite. The technique is fully described by Manders [25]. A ~ 3 mm thick slice is bonded to an anode block with conducting cement and its other polished

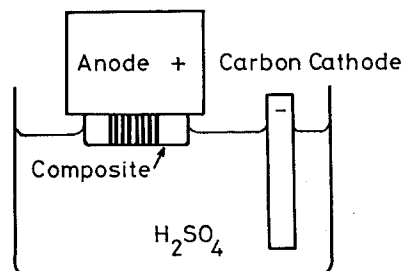


Figure A1 The method of electrolytically decorating conducting fibres in sections of composite.

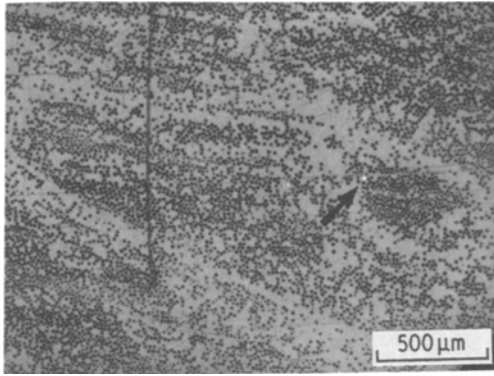


Figure A2 Electrolytically decorated section of a carbon fibre composite strained to failure (0.013) showing a single non-conducting fibre (bright, and arrowed).

surface is etched in H_2SO_4 to develop colouration on the ends of fibres which are electrically connected to the anode. The colouration is due to the formation of a graphite intercalation compound (graphite bisulphate) and provides good contrast with the unconnected fibres which retain their bright polish, see Fig. A1. Because the fibres are misaligned, there are conduction paths between fibres, and fractures some distance from the surface are electrically bridged and cannot be detected. In practice, at 0.6 volume fraction,

fractures in the top $100\mu m$ or so effectively isolate the fibre ends [24].

When applied to all-carbon fibre composites, the technique shows that a composite strained to failure has very few fibre fractures, see Fig. A2, and these are single fractures, indicating a critical group size of two fibres. Analysis of a number of such micrographs suggests a maximum density of fibre fractures of the order of $10^{10} m^{-3}$. This corresponds to about one every 4m on a single fibre, although some were certainly introduced at the fabrication stage or earlier. The total number detected is too small to accurately determine the rate of fibre fracture with straining. A better measure of this is acoustic emission which was discussed in Part 1 [1].

In hybrid composites, where the ligaments of cfrp are smaller, and where multiple cracking is possible, much higher strains may be sustained before ultimate failure of the composite, and there is a significant increase in the density of fibre fractures. Fig. A3 shows two decorated cross-sections of spread-tow hybrids which have been taken to successively higher strains. The rapid increase in the number of fractures with strain, and their tendency to be grouped is clearly seen. At low strains individual fractures, and groups of

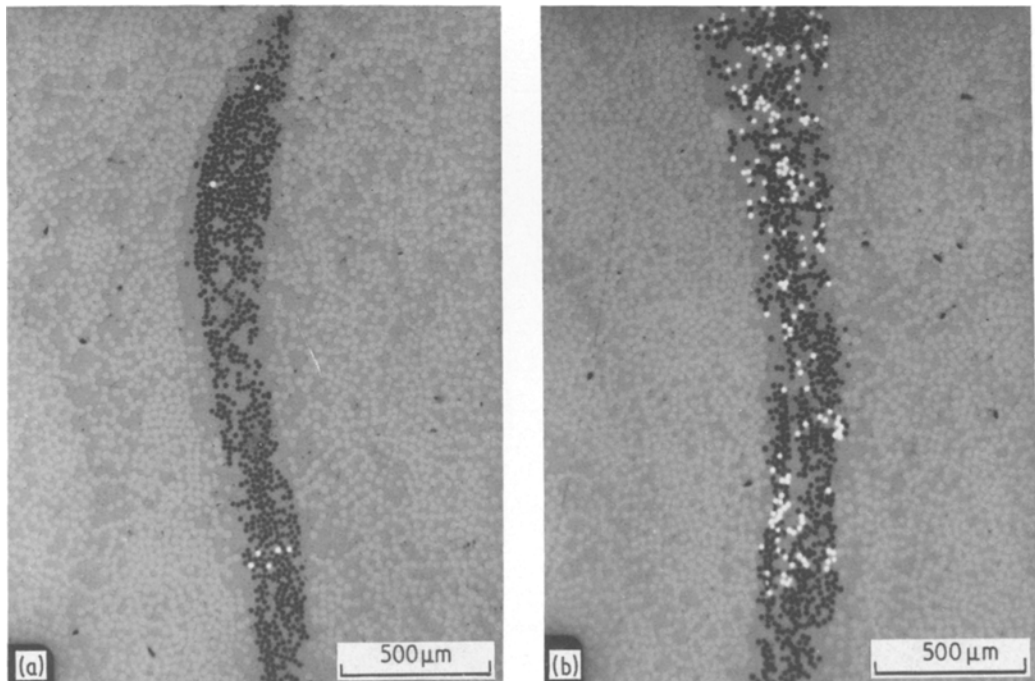


Figure A3 Electrolytically decorated sections of spread-tow hybrids strained to (a) 0.020 and (b) 0.023. Unbroken carbon fibres appear black, broken fibres white, and glass fibres grey.

2 or 3 predominate, whereas at higher strains the groups are larger, and ultimately are limited by the size of the groups which constitute the layer of fibres (because of uneven distribution).

Overall, these observations validate a model of fracture in which individual fractures of carbon fibres cause overstress in neighbouring fibres over some distance approximating to the length of debonding between fibre and matrix. Fracture then propagates fibre-by-fibre until a critical group of about 2 to 3 fibre fractures is reached, when it becomes catastrophic.

References

1. P. W. MANDERS and M. G. BADER, *J. Mater. Sci.* **16** (1981) 2233.
2. R. MORTON, PhD Thesis, University of Surrey (1977).
3. J. D. H. HUGES, H. MORLEY and E. E. JACKSON, *J. Phys. D, Appl. Phys.* **13** (1980) 921.
4. B. D. COLEMAN, *J. Mech. Phys. Sol.* **7** (1958) 60.
5. D. GÜÇER and J. GURLAND, *ibid.* **10** (1962) 365.
6. B. W. ROSEN, *J. AIAA.* **2** (1964) 1985.
7. C. ZWEBEN, *ibid.* **6** (1968) 2325.
8. C. ZWEBEN and B. W. ROSEN, *J. Mech. Phys. Sol.* **18** (1970) 189.
9. B. W. ROSEN, *Proc. Roy. Soc. Lond. A.* **319** (1970) 79.
10. B. W. ROSEN and C. H. ZWEBEN. NASA CR-2057, 1972.
11. C. ZWEBEN, *Eng. Fract. Mech.* **4** (1972) 1.
12. P. M. SCOP and A. S. ARGON, Conference Proceedings of Advanced Fibrous Reinforced Composites, (SAMPE, San Diego, Calif. 1966).
13. *Idem*, *J. Comp. Mater.* **3** (1969) 30.
14. A. S. ARGON, in "Composite Materials: Fracture and Fatigue", Vol. 5, edited by L. J. Broutman (Academic Press, London and New York) p. 153.
15. D. G. HARLOW and L. S. PHOENIX, *J. Comp. Mater.* **12** (1978) 195, 314.
16. S. B. BATDORF, private communication, 1980.
17. J. AVESTON and J. M. SILLWOOD, *J. Mater. Sci.* **11** (1976) 1877.
18. M. G. BADER and P. W. MANDERS, Proceedings of the 2nd International Conference on Composite Materials, (AIME, New York, 1978) pp. 1147-65.
19. J. M. HEDGEPEETH, NASA Technical note D-882, 1961.
20. J. M. HEDGEPEETH and P. VAN-DYKE, *J. Comp. Mater.* **1** (1967) 294.
21. P. VAN-DYKE and J. M. HEDGEPEETH, *Textile Res. J.* **39** (1969) 619.
22. W. L. KO, *J. Comp. Mater.* **12** (1978) 97.
23. C. ZWEBEN, *J. Mater. Sci.* **12** (1977) 1325.
24. P. W. MANDERS, PhD Thesis, University of Surrey, 1979.
25. *Idem*, *Nature* **271** (1978) 142.
26. R. L. SMITH, *Proc. Roy. Soc.* **A372** (1980) 539.
27. D. G. HARLOW and S. L. PHOENIX, *Int. J. Fracture* **15** (1979).

Received 9 December 1980 and accepted 5 February 1981.